F-3-1L
Extended Abstracts of the 2009 International Conference on Solid State Devices and Materials, Sendai, 2009, pp832-833

# Effect of Electrode Contacts on Transport in Carbon Nanofiber Interconnects

Hisashi Yabutani[1], Toshishige Yamada[1], Saito Tsutomu[2], and Cary Y. Yang[1]

[1]Santa Clara University, Center for Nanostructures
500, El Camino Real, Santa Clara, California 95053-0569, U.S.A.
Phone: +1-408-554-6817 E-mail: HYabutani@scu.edu
[2]Hitachi High-Technologies Corporation,
882 Ichige, Hitachinaka, Ibaraki 312-8504, Japan

## 1. Introduction

Carbon nanofibers (CNFs) are one of the most promising materials for next-generation on-chip interconnects due to their demonstrated high current capacities and immunity to electromigration [1], [2]. The critical issue of achieving optimal resistance for carbon-based interconnects is of the utmost interest to researchers in the field. In this paper, we report the effect of electrode contacts on the total resistance and electrothermal transport behavior of CNF interconnects.

## 2. Experiments and Heat Transport Model

CNFs used in these measurements were grown using plasma-enhanced chemical vapor deposition technique with Ni catalyst [2]. These CNFs were dispersed onto a $SiO_2$ substrate of pre-patterned gold (Au) electrodes after immersing in isopropyl alcohol. Subsequently, using focused ion beam technique, tungsten (W) was deposited to form two types of electrodes bridging CNF [3]. Fig. 1 shows the top and side views of scanning electron microscope (SEM) images of a single CNF (sample A) between W-deposited electrode contacts. Since the entire CNF rests on the $SiO_2$ substrate, the deposited W is connected to the Au electrode to facilitate electrical measurements. We use a bright contrast technique to confirm that the CNF is indeed completely supported by the substrate [4]. Fig. 2 shows a CNF with both ends resting on Au electrodes and deposited W, forming a pair of W-Au electrode contacts (sample B).

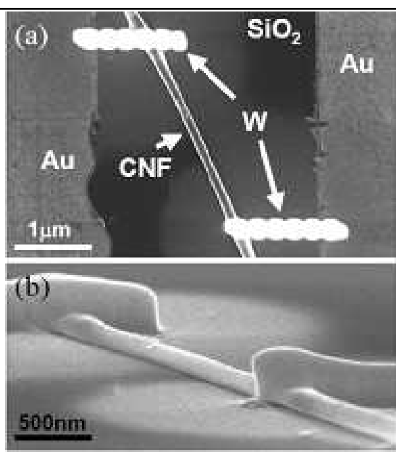


Fig. 1 (a) SEM image of Sample A, fully supported on $SiO_2$ substrate. FIB-deposited W connects CNF to Au electrode. (b) Side view showing CNF between W-deposited contacts.

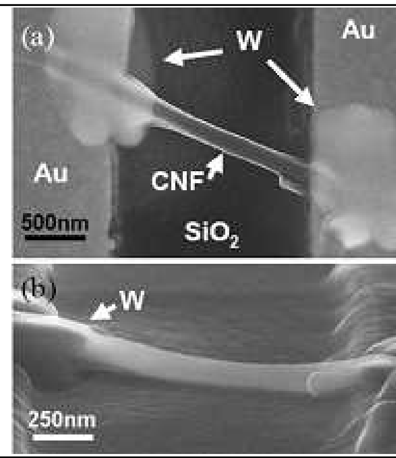


Fig. 2 (a) SEM image of Sample B, showing both ends of CNF on Au electrodes with deposited W. (b) Side view showing the left end of CNF covered by W.

Between these contacts, the CNF is completely supported by the $SiO_2$ substrate.

Stress current is applied to these two samples progressively, *i.e.*, in the first cycle, a small current is applied for three minutes, and in the second cycle, a larger current is applied for another three minutes, etc. We monitor the voltage change during each stress cycle until breakdown occurs. Fig. 3 shows the total resistance, $R_{tot}$, which is the average voltage divided by stress current during each cycle, versus stress current density, $J_s$. Fig. 3 shows a decrease in $R_{tot}$ with increasing $J_s$ for both samples. Since increase in $J_s$ gives rise to increase in Joule heating, the empirical relationship in Fig. 3 can be regarded qualitatively as the behavior of CNF resistance versus temperature. To obtain a quantitative relationship, it is necessary to study the relationship between stress current and temperature.

Our one-dimensional heat transport model takes into account Joule heat generation by stress current, dissipation to $SiO_2$ substrate/electrode, and diffusion [5]. The model assumes that the type of contact with CNF defines the extent of heat dissipation at that interface, and that breakdown occurs when the peak temperature, $T_{max}$, reached a critical or threshold temperature, $T_{th}$, at which carbon atoms starts to evaporate [6]. This model allows us to relate stress current with temperature and to generate a temperature distribution profile along the CNF length, as we reported previously [5].

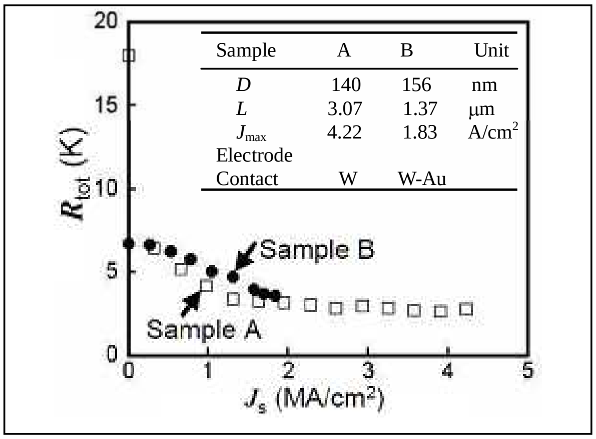


Fig. 3 Total resistance versus stress current density. Properties of CNF samples are given in inset.

Fig. 4(a) shows an SEM image of sample A after breakdown. The fact that an open circuit is observed at breakdown confirms that the lateral spread of deposited W has not resulted in shorting of the device. For this device, the CNF is fully supported on the substrate throughout, including the W-deposited segments. Therefore, we neglect heat diffusion and assume uniform heat dissipation along the entire CNF length. The resulting temperature profile from our heat transport model [5] is shown in Fig. 4(b).

For sample B, shown in Fig. 5, breakdown occurs over a wide range near the middle of the substrate-supported segment. Since the heat dissipation at W-Au electrodes is considerably larger than that through the $SiO_2$ substrate, the temperature at the electrodes is expected to be lower than in the supported segment. Fig. 5(b) shows the corresponding temperature profile, obtained using our heat transport model [5].

Breakdown in sample A occurs at $J_s$ = 4.3 MA/cm$^2$, and in sample B at 1.9 MA/cm$^2$. The difference in maximum $J_s$ at breakdown is attributed to difference in electrode contacts. The CNF in sample A is placed on the flat $SiO_2$ surface with W-deposited electrode contacts, while the CNF in

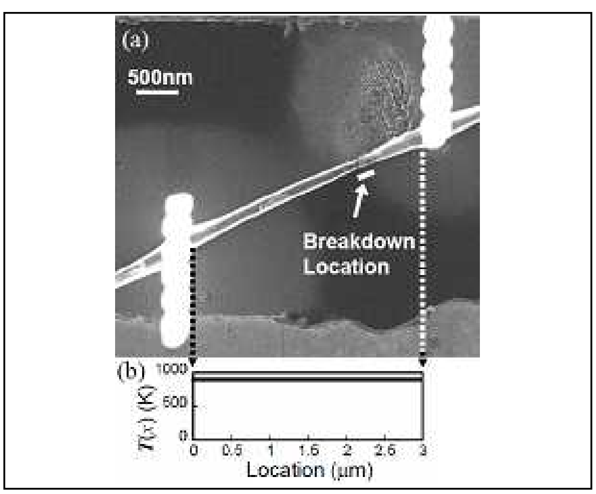


Fig. 4 (a) SEM image of Sample A after breakdown. (b) Calculated temperature profile using heat transport model [5].

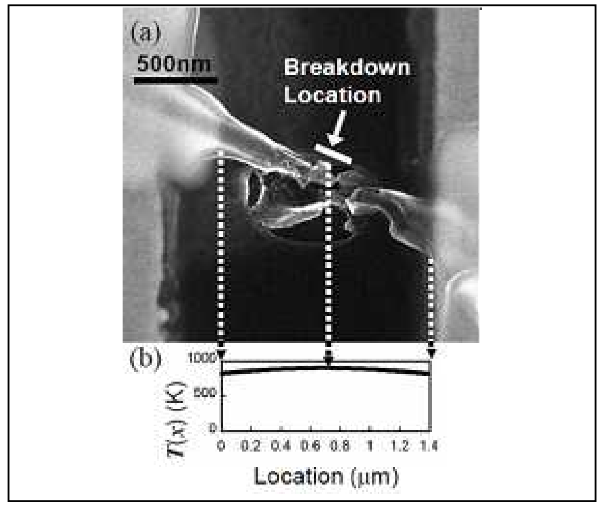


Fig. 5 (a) SEM image of Sample B after breakdown. (b) Calculated temperature profile using heat transport model [5].

sample B rests between two W-Au electrodes (thickness of Au film = 100 nm). Although sample A is more than twice as long, which usually results in lower current capacity [3], heat dissipation in sample A is more efficient than in sample B due to its contact geometry with both substrate and electrodes. Further, the mechanical stress introduced by the bending of CNF near both ends in sample B is expected to lessen its tolerance to Joule heating. In fact, this stress is a probable cause for the seemingly catastrophic breakdown as shown in Fig. 5.

## 3. Conclusion

We have examined the transport in CNF interconnects with two types of electrode contacts, using current stress measurements and a heat transport model. The difference in maximum current density is attributed to structural differences in the electrode contacts.


## Acknowledgements

This work was supported by the United States Army Space and Missile Defense Command (SMDC) and carries Distribution Statement A, approved for public release, distribution unlimited.


## References


[1] M. Nihei, A. Kawabata, D. Kondo, M. Horibe, S. Sato, and Y. Awano, Jpn. J. Appl. Phys., **44** (2005) 1626.

[2] B. A. Cruden, A. M. Cassell, Q. Ye, and M. Meyyappan, J. Appl. Phys. **94** (2003) 4070.

[3] T. Saito, T. Yamada, D. Fabris, H. Kitsuki, P. Wilhite, M. Suzuki, and C. Y. Yang, Appl. Phys. Lett., **93** (2008) 102108.

[4] M. Suzuki, T. Yamada, and C. Y. Yang, Appl. Phys. Lett., **90** (2007) 083111.

[5] T. Yamada, T. Saito, D. Fabris, and C. Y. Yang, IEEE Electron Device Lett., **30** (2009) 469.

[6] K. Hata, D. N. Futaba, K. Mizuno, T. Namai, M. Yumura, and S. Iijima, Science, **306** (2004) 1362.